Supplemental Document

Optics Letters

Wavelength beam-combining of terahertz quantum-cascade laser arrays: supplement

JI CHEN,[1,3] YUAN JIN,[1] LIANG GAO,[1] JOHN L. RENO,[2] AND SUSHIL KUMAR[1,4]

[1]*Department of Electrical and Computer Engineering, Lehigh University, Bethlehem, Pennsylvania 18015, USA*
[2]*Sandia National Laboratories, Center of Integrated Nanotechnologies, MS 1303, Albuquerque, New Mexico 87185-1303, USA*
[3]*e-mail: jic615@lehigh.edu*
[4]*e-mail: sushil@lehigh.edu*

Supplement DOI: https://doi.org/10.6084/m9.figshare.14229911

Parent Article DOI: https://doi.org/10.1364/OL.420398

Wavelength beam-combining of terahertz quantum-cascade laser arrays

Supplementary Information

1. MATERIALS AND METHODS

Fabrication of QCLs

The active-medium of the THz-QCLs is based on a three-well resonant-phonon design with GaAs/$Al_{0.15}Ga_{0.85}As$ superlattice (design RT3W221YR16A, wafer number VB0832, with layer widths (starting from the injector barrier) of **57**/18.5/ **31**/9/**28.5**/16.5 monolayers (ML, 1 ML = 2.826 Å)). The superlattice was grown by molecular-beam epitaxy (MBE), with 221 cascaded periods, leading to an overall thickness of 10 μm. Cu-Cu based metallic waveguides were fabricated using standard THz QCL fabrication techniques with thermocompression wafer bonding. Distributed-feedback (DFB) ridge cavities were processed by wet-etching, where the grating periodicity was defined lithographically. Details related to the MBE growth sequence and DFB QCL fabrication sequence that included implementation of lateral and longitudinal absorbing sections in the cavities to suppress undesired higher order cavity modes are described in Ref. [1].

Fabrication of HDPE lens

The plano-convex HDPE lenses were sawed manually from 1-inch diameter commercial HDPE balls (from Precision Plastic Ball Co.). The cutting interface was polished to form a flat circular plane by a lapping machine. The thickness of different lenses was varied by controlling the lapping time. The lens was mounted in front of the TPX window of Stirling cryocooler by using home-made brass mounts.

Fabrication of blazed grating

The blazed grating was made using a high-resolution in-house CNC milling machine (Othermill Co.). The milling resolution of this machine is 10 μm. A flat brass plate was attached on the surface of a tilted brass substrate. The tilt-angle of the substrate is 21.8°, which is same as the blazed angle of grating. The attached brass plate is milled by a flat-end tip moving in one direction with a depth of 60 μm. After finishing one groove in this direction, the tip is set to move in the vertical direction with a step of 150 μm and mill the next groove. Finally, a grating with 60 μm $\times$ 150 μm right-angled triangular grooves was realized on a 1 in.$\times$ 1 in. brass plate.

Measurements

A cleaved chip consisting of DFB QCLs was indium soldered on a copper block, the QCL to be tested was wire-bonded for electrical biasing, and the copper block was mounted on the cold-stage of the Stirling cryocooler. A 530 μm thick TPX window was used in the vacuum chamber to couple THz radiation outside of the cryocooler for measurements. The QCL was biased with 200 ns wide rectangular current pulses repeated at 100 kHz at a heat-sink temperature of 62 K. Far-field beam patterns were measured with a THz pyroelectric detector (Gentec THz 2I-BL-BNC, element size 2 mm $\times$ 2 mm) mounted on a 2D motorized scanning stage. The absolute power was calibrated using a thermopile power meter (Scientech AC2500 with AC25H) and is reported without any corrections to the detected signal. Laser spectra were measured using a Fourier-transform infrared spectrometer (Bruker Vertex 70v).

2. DESIGN OF WAVELENGTH BEAM COMBINING SYSTEM

Design of optical elements and lithographic design of QCLs

As mentioned in the manuscript, the lasers and optical elements are designed to achieve the goal of same output angles while balancing the different locations and frequencies of lasers. QCLs around the peak gain frequency of 3.3 THz were lithographically designed with a frequency spacing of 0.08 THz, by varying the grating period of the Bragg gratings on top of the metallic

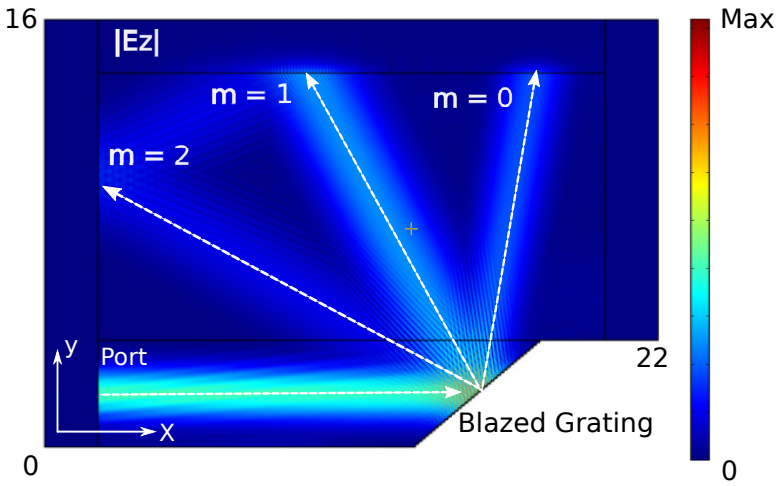

Fig. S1. Norm of the z-polarized electric-field computed using two-dimensional FEM simulation of the blazed grating. The grating geometry parameters are the same as that in main text, and the rotation angle is set to be 50° as per the experimental configuration. The incident radiation is a 3.39 THz fundamental Gaussian beam that propagates along x with a FWHM divergence of 1° (from the left port). The electric-field is polarized in the z direction in accordance with the polarization of DFB THz QCLs in the experimental setup.

QCL cavities. The center-to-center spacing between neighboring QCLs was set to 0.5 mm, based on the fabrication convenience. It should be larger than the width of laser ridge (0.2 mm), but not too large to save wafer space. The custom-made HDPE lens is used to collimate the beams from QCLs with a high power efficiency [2]. Once these parameters are determined, a blazed grating was designed considering an optimal grating rotation angle (as shown in see Fig. 3e of main text) to achieve a minimum angular deviation based on the Eq. 2 in the main text. In order to have a high first-order ($m = 1$) diffraction-efficiency for P plane-wave as for DFB QCLs in this experiment, the grating period with an optimal λ/d value of ~ 0.6 was implemented, which is close to the ratio with peak-efficiency of this grating [3]. The grating grooves have to be right-angled because of the flat-end milling tip in fabrication. The edge length is 60 μm$\times$150 μm which is also based on the considerations of the resolution of the CNC milling machine (10 μm). Based on finite-element method (FEM) simulation using COMSOL [4], the diffraction efficiencies of this blazed grating were computed and are shown in Fig. S1. Incident radiation (frequency 3.39 THz) and reflected beams corresponding to three diffraction orders ($m = 0, 1, 2$) are shown in the figure (the directions are marked by the white dashed lines). In WBC, first-order diffraction is used, which has as power efficiency of 65% in the simulation.

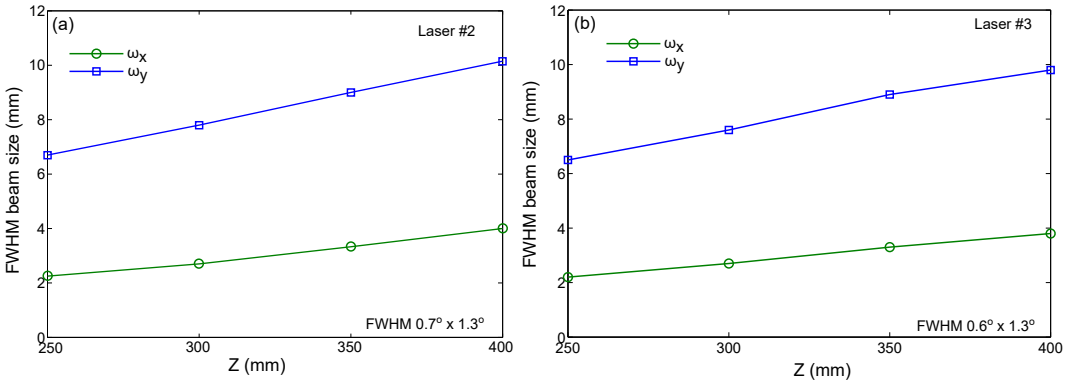

Fig. S2. FWHM beam size of (a) QCL #2, and (b) QCL #3 in x and y directions respectively. The estimated value of the FWHM divergence angle by curve-fitting is indicated on the plots.

Beam sizes after lens

The variation of beam's size in x and y directions after the lens as the beam propagates are due to the focusing characteristics of the lens and the fact that the original quasi-Gaussian beam from the QCLs has elliptical symmetry. This behavior was described in detail in Ref. [2]. Because the distance from lens to QCLs is the focal length of lens, each beam after lens is collimated with a small divergence angle. Beam patterns at increasing distances (Z) after lens are measured. Fig. S2 shows the FWHM beam sizes of QCL #2 and #3, in x and y directions respectively. With linear curve-fitting of the beam-size curves, far-field FWHM divergence of $\sim 1^\circ \times 1^\circ$ is estimated.

Beam sizes after combining

Beam patterns at increasing distances after combining are also measured. Fig. S3 shows the beam patterns and their FWHM beam sizes of QCL #3, in x and y directions respectively. With linear curve-fitting of the beam-size curves as shown in Fig. S3(b), far-field FWHM divergence of $\sim 1^\circ \times 1^\circ$ is estimated.

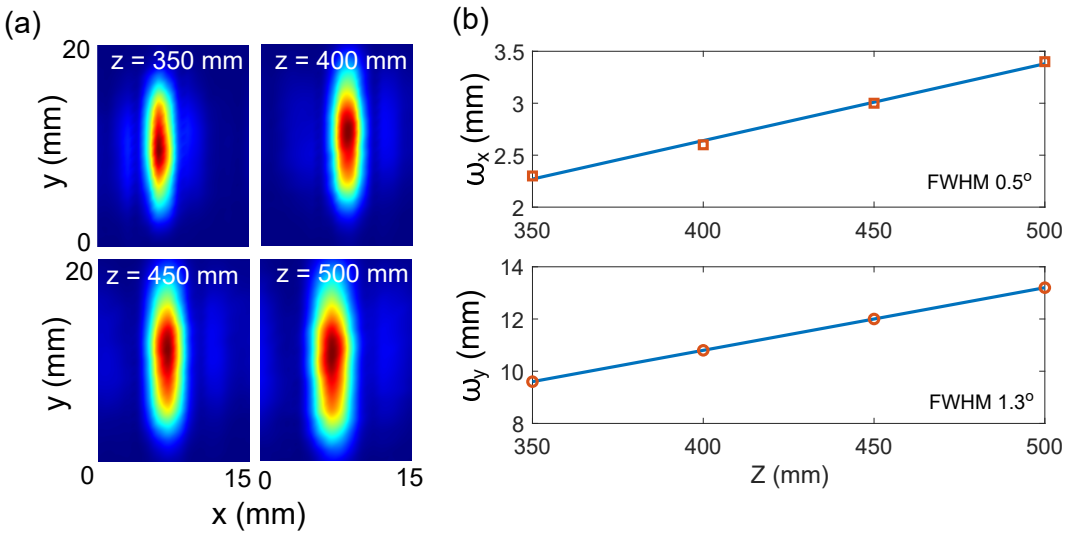

Fig. S3. (a) Beam patterns of QCL #3 after combining at z = 350 mm, 400 mm, 450 mm and 500 mm. (b)FWHM beam size QCL #3 after combining in x and y directions respectively. The estimated value of the FWHM divergence angle by curve-fitting is indicated on the plots.

REFERENCES

1. Y. Jin, L. Gao, J. Chen, C. Wu, J. L. Reno, and S. Kumar, "High power surface emitting terahertz laser with hybrid second-and fourth-order bragg gratings," Nat. Commun. **9**, 1407 (2018).
2. J. Chen, L. Gao, Y. Jin, J. L. Reno, and S. Kumar, "High-intensity and low-divergence THz laser with 1D autofocusing symmetric airy beams," Opt. Express **27**, 22877–22889 (2019).
3. E. Loewen, M. Nevière, and D. Maystre, "Grating efficiency theory as it applies to blazed and holographic gratings," Appl. Opt. **16**, 2711–2721 (1977).
4. COMSOL 4.4, a finite-element partial differential equation solver from COMSOL Inc.